the rings are closed at condensation temperature in the range 310–345 °C after 4 h but are not completely aromatized. However, a large number of rings remain open if the polymer is condensed at 250 °C. The final ladder polymer is very stable toward temperature, air, acids, and base. It is soluble in strong acid if it is polycondensed below 385 °C and partly soluble when condensed at that temperature.

The regular one-dimensional packing of PMQ when precipitated from H_2SO_4 implies that it has a regular structure. If nitrogen were lost, ring closure would give five-membered rings which would change the polymer shape and inhibit stacking. Loss of nitrogen without ring closure would prevent all stacking. It seems probable then that nitrogen is not lost but that the element analysis cannot recover all of it in this refractory polyaromatic compound. We conclude that we probably have truly synthesized PMQ.

Acknowledgment. This work was partly supported by Dow Chemical Co., DOE, and the National Science Foundation.

Registry No. PMQ, 104491-01-2; $((2,6\text{-}NH_2)_2C_6H_3CH_3)(CH_2O)$ (copolymer), 112265-13-1; $((2,6\text{-}NH_2)_2C_6H_3CH_3)(CH_2O)$ (copolymer, SRU), 112265-22-2.

References and Notes

(1) Ivory, D. M.; Miller, G. G.; Sowa, J. M.; Shacklette, L. W.; Chance, R. R.; Baughman, R. H. *J. Chem. Phys.* **1979**, *71*, 1506.
(2) Rabott, J. F.; Clarke, T. C.; Kanazawa, K. K.; Reynolds, J. R.; Street, G. B. *J. Chem. Soc., Chem. Commun.* **1980**, 347.
(3) Shacklette, L. W.; Elsenbaumer, R. L.; Chance, R. R.; Sowa, J. M.; Ivory, D. M.; Miller, G. G.; Baughman, R. H. *J. Chem. Soc., Chem. Commun.* **1982**, 361.
(4) Druy, M. A.; Rubner, M. F.; Walsh, S. P. *J. Electrochem. Soc. Ext. Abs.* **1984**, *84*, 617.
(5) Shacklette, L. W.; Eckhardt, H.; Chance, R. R.; Miller, G. G.; Ivory, D. M.; Baughman, R. H. *J. Chem. Phys.* **1980**, *73*, 4098.
(6) Shacklette, L. W.; Chance, R. R.; Ivory, D. M.; Miller, G. G.; Baughman, R. H. *Synth. Met.* **1984**, *1*, 307.
(7) Shacklette, L. W.; Elsenbaumer, R. L.; Chance, R. R.; Eckhardt, H.; Frommer, J. E.; Baughman, R. H. *J. Chem. Phys.* **1981**, *75*, 1919.
(8) Tessler, M. M. *Polym. Prepr. (Am. Chem. Soc., Div. Polym. Chem.)* **1967**, *8*, 165.
(9) Baughman, R. H. *J. Polym. Sci., Polym. Lett. Ed.* **1983**, *21*, 475.
(10) Tanaka, K.; Ohzehi, K.; Yamabe, T.; Yata, S. *Synth. Met.* **1984**, *9*, 41.
(11) Ruan, J. Z.; Litt, M. H. *J. Polym. Sci., Polym. Chem. Ed.* **1987**, *25*, 299.
(12) Ruan, J. Z.; Litt, M. H. *J. Polym. Sci., Polym. Chem. Ed.* **1987**, *87*, 285.
(13) Kharas, G. B.; Litt, M. H. *J. Polym. Sci., Polym. Chem. Ed.* **1984**, *22*, 1231.
(14) Snyder, H. R.; Konecky, M. S. *J. Am. Chem. Soc.* **1958**, *80*, 4388.
(15) Elbs, K.; Wohlfahrt, *J. Prakt. Chem.* **1898**, *2*, 536.
(16) Burke, W. J.; Ruetman, S. H. *J. Polym. Sci.* **1958**, *32*, 221.
(17) Cocq, C. L.; Lallemand, J. V. *J. Chem. Soc., Chem. Commun.* **1981**, 150.
(18) Levy, G. C.; Lichter, R. L.; Nelson, G. L. *Carbon-13 Nuclear Magnetic Resonance Spectroscopy*; Wiley: New York, 1980.
(19) Silverstein, R. M.; Bassler, G. C.; Morrill, T. C. *Spectrometric Indentification of Organic Compounds*: Wiley: New York, 1980.
(20) Bailey, M. L. *Chem. Heterocycl. Compd.* **1973**, *9*, 631.
(21) Stern, E. S.; Timmons, C. J. *Electronic Absorption Spectroscopy in Organic Chemistry*; Edward Arnold LTD: London, 1970.
(22) Kissman, H.; Farnsworth, D.; Witkop, B. *J. Am. Chem. Soc.* **1952**, *20*, 3948.
(23) Idelson, A. L.; Litt, M. H. U. S. Patent, 3-535-284, 1970.
(24) Kim, O. K. *J. Polym. Sci., Polym. Lett. Ed.* **1985**, *23*, 137.
(25) *Tables of Interatomic Distances and Configuration in Molecules and Ions*; Supplement, 1956–1959, Special Publication No. 18, London, The Chemical Society, 1965. For C=N in phenazine and acridine, d = 1.345 Å. For C=C in polyaromatics such as acridine, d = 1.39 Å.
(26) Wycoff, R. W. G. *Crystal Structures*; Oxford University Press: London, 1962; Vol. I, p 26.
(27) Stadler, H. P. *Acta Crystallogr.* **1953**, *6*, 540.
(28) Ten, T. F.; Erdman, J. G.; Pollack, S. S. *Anal. Chem.* **1961**, *33*, 1587.
(29) Cullity, B. D. *Elements of X-ray Diffraction*; Addison-Wesley: 1978; p 102.

Electronic Properties of Poly(1-methylcyclohexa-1,3-diene-2,3-diyl-5,6-diylidene-5-methylidyne-6-nitrilo)

J. Z. Ruan and M. H. Litt*

Department of Macromolecular Science, Case Western Reserve University, Cleveland, Ohio 44106. *Received June 27, 1986*

ABSTRACT: Poly(1-methylcyclohexa-1,3-diene-2,3-diyl-5,6-diylidene-5-methylidyne-6-nitrilo) (PMQ), prepared at four different temperatures from 250 to 385 °C, was studied. There is 1 spin per 200 to 400 repeats. The temperature dependence of unpaired spin concentration for PMQ4 condensed at 385 °C implies that a phase transition from magnetic disorder to order may occur near 74 K. PMQ3 condensed at 345 °C was doped with nitrosyl hexafluorophosphate (NFP) and iodine. Iodine intercalated between the layers but hexafluorophosphate did not. EPR studies suggest that NO^+ oxidized the polymer to produce charged spinless species. There is strong coupling between iodine nuclei and the spin system. The as is conductivities at 25 °C range from about 10^{-11} S/cm for PMQ1 condensed at 250 °C to 2×10^{-5} S/cm for PMQ4 condensed at 385 °C. The conductivity of PMQ3 increases by 6 and 7 orders of magnitude upon doping with NFP and iodine, respectively, to a high of 2.4×10^{-2} S/cm at 21 °C.

Introduction

Although a large number of conducting polymers have been discovered in recent years,[1-4] the electronic structures of the doped polymers are not well understood. Perhaps the most important difference between organic and inorganic semiconductors is the influence of the lattice structure on charge transport. Polyacetylene is a typical example of the Peierls distortion in a linear chain[5,6] involving the π-electrons at half-filled band level. An additional hole or electron will be accommodated by soliton distortion[7,8] in the bond alternation of the polyacetylene chain. As a carrier or soliton moves through the polymer

0024-9297/88/2221-0882$01.50/0

it carries along this distortion, hence lowering its mobility. In inorganic semiconductors the distortion is much less; the mobility can thus be very high, close to 10^5 cm^2/V s.[9]

Polyacene, a structure much studied theoretically, is one of the simplest members of the polymer class consisting of two polyacetylene chains joined by crossties. Salem et al.[10] concluded that no Peierls distortion in polyacene is expected in the framework of Hückel CO (crystal orbital) theory. In addition, sufficiently long polyacene chains have been predicted to become either ferromagnetic or antiferromagnetic, or they may have high-temperature superconductivity.[11,12]

The ladder aromatic polymer poly(1-methylcyclohexa-1,3-diene-2,3-diyl-5,6-diylidene-5-methylidyne-6-nitrilo) (PMQ),[13] reported on this paper, is one of the closest to the polyacene structure which has been made. PMQ has

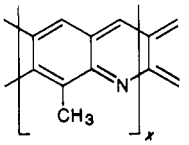

PMQ

a backbone with a highly conjugated planar configuration. The π-electrons in the backbone should be fully delocalized along the chain. The side methyl group makes π-electrons in the backbone more reactive toward electron acceptors, which facilitates doping. The backbone has two isomers, each of which has doubly degenerate states: Tanaka et

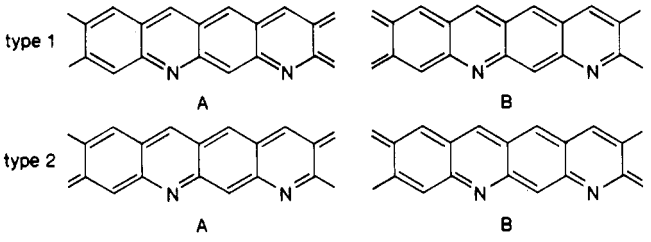

al. have reported that for linear polyacene, the type 2 isomer is about 0.13 kcal/mol more stable than the type 1 isomer. In contrast to polyacetylene, a radical, cation, or anion defect on the backbone will divide the polymer into a type 1 and a type 2 section. Therefore, a soliton

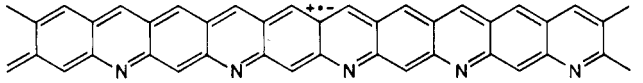

model is not favored here because the two sides do not have the same energy, even though the backbone has doubly degenerate ground states. However, a polaron or bipolaron will divide the polymer into two energetically equivalent ground-state structures. Hence, it can move

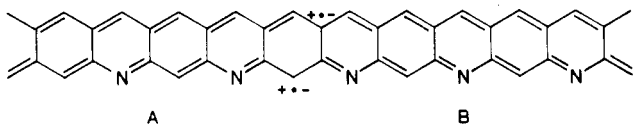

in either direction without affecting the energy on the backbone, assuming a highly idealized situation of infinite chain length.

However, the backbone is bent in the plane because the C=N bond length is about 0.05 Å shorter than that of the C=C.[13] Thus the molecules can stack on top of each other very well, but the stacks cannot pack well into each other. In fact, if the chains are long enough (DP $\simeq$ 75), the molecules would form a circle or helix. This makes if very difficult to pack the stacks together in a fashion which generates good intermolecular contacts. This paper details the characterization of some of the structural and electronic properties of the undoped and doped PMQ.

Table I
Element Analysis of NFP- and Iodine-Doped PMQ3

	C	H	N	P	I
found PMQ3 (NFP doped)	43.24	3.63	6.21	9.72	
calcd 97.5% (C_8H_5N·0.70PF_6)	43.25	2.27	6.30	9.77	
found PMQ3 (I_2 doped)	33.33	2.02	3.46		50.35
calcd[a] $C_8H_5N_{0.71}I_{1.14}$ + 0.5H_2O·0.02HPO_3·0.21H_2SO_4	33.42	2.24	3.36		50.40

[a] Polyphosphoric and sulfuric residues are included because they were found in the undoped polymer.[13]

Experimental Section

The synthetic procedure used to prepare the polymer under investigation was discussed in the previous paper.[13] 2,6-Diaminotoluene reacts with formaldehyde in aqueous solution with acid catalysts to produce a prepolymer, which through further condensation in poly(phosphoric acid) at high temperature produces the final polymer. Four polymers—PMQ1, condensed at 250 °C; PMQ2, condensed at 310 °C; PMQ3, condensed at 345 °C; and PMQ4, condensed at 385 °C—were studied. PMQ3 was doped with nitrosyl hexafluorophosphate (NFP), $NOPF_6$, and iodine.

Doping with NFP. NFP (1.0 g) (Alfa Chemicals) was dissolved in 50 mL of nitromethane, 0.60 g of PMQ3 was then added, and the suspension was stirred for 2 h. The dopant solution was removed by centrifuging and filtering, using a fine-fritted glass filter. The doped polymer was washed 4 times with clean nitromethane to remove residual dopant and dried in a vacuum oven at room temperature for 2 h. One-quarter of the doped polymer was taken for IR, X-ray, and conductivity measurements; the remainder was doped again as described above. PMQ3 was partly soluble and measurements were run on the doped insoluble fraction. The amount of dopant was determined from element analysis (Galbraith Laboratories, Inc.).

Doping with Iodine. Finely powdered PMQ3 (0.25 g) was put into a coarse-fritted glass filter which was set beside another coarse-fritted glass filter containing iodine inside a vacuum desiccator containing Drierite. Vacuum was applied. The polymer was weighed every 2 weeks. After about 2.5 months, the weight became constant. The iodine concentration in doped PMQ was determined both from weight increase and from element analysis. Table I lists the element analyses of NFP and iodine-doped PMQ3.

The found values for NFP doped PMQ3 fit quite well with the calculated ones. The value of 97.5% is used sinced it is the sum of all elements in the doped polymer assuming that F is present as PF_6^-. Since a solvent was used for doping, much of the H_2SO_4 etc. must have been removed by extraction. The residue could be ash and/or H_2SO_4. The phosphorus potentially contributed by the residual HPO_3 is too small to be important. It is a maximum of 0.024P per residue compared to the 0.70P per residue in the doped polymer. The found carbon/nitrogen ratio in iodine-doped PMQ3 is about the same as for undoped PMQ3.[13]

X-ray Diffraction and IR Spectra. X-ray diffractions were done on a Philips automated powder diffractometer with monochromatized Cu Kα radiation. It was scanned at 1.2 deg min^{-1} with a 0.02-deg step. IR spectra of doped polymer KBr pellets were recorded on a Digilab FTS-14 FTIR spectrometer at a resolution of 4 cm^{-1} with a total of 50 scans.

Electron Paramagnetic Resonance Measurements. EPR spectra were taken on a Varian E-112 X-band spectrometer with a E-238 cavity and E-258 variable-temperature accessory for E-line series. The spectra were stored in the system memory for further analysis. Double integration was used to calculate the signal intensity. At all temperatures, the powder level was set at 1 mW, well below the spin saturation. A 100-KHz magnetic field was applied as modulation. Diphenylpicrylhydrazyl (DPPH), g = 2.0037, was used as a reference to calibrate the g factor and spin concentration.[15] One and a half milligrams of DPPH (Aldrich) was mixed with 400 mg of KBr, 20.0 mg of which was transfered

to EPR tube after thorough grinding. The tube was kept in a vacuum desiccator until used. A narrow Lorentzian line shape (ΔH_{pp} = 2.5G) was found for the DPPH, indicating that the DPPH had not degraded and was reliable for calibration. Temperature dependence of unpaired spin density was determined in the range of 80 to 450 K. The low temperature was achieved by letting nitrogen gas flow through a coil of copper tubing immersed in liquid nitrogen before entering the resonance cavity. The temperatures were measured by using a copper–constantan thermocouple adjacent to the sample, with a 0 °C reference. Thermopotential was displayed on a Keithly 177 Microvolt DMM. Vacuum was applied to remove oxygen. The spin–lattice relaxation times were obtained by using EPR saturation technique. The microwave magnetic field H_1 in the cavity was determined by the method of perturbing spheres[16] and is given in Gauss by[17]

$$H_1^2 = 0.204W \quad (1)$$

where W is the Klystron power in watts.

Electronic Conductivity Measurement. Four platinum wires were sealed with epoxy in a square configuration 3.5 mm apart in a glass inner adaptor. The platinum wires were joined with copper wires, two of which connected to a constant current supply (Keithley 220 programmable current source) and the other two to the voltmeter (Keithley 192 programmable DMM). conductivities were calculated by using eq 2[18] for the four-point square

$$\sigma = (\ln 2)I/(2\pi aV) \quad (2)$$

probe, which is accurate provided that the sample thickness a is much smaller than the square dimension. A 13 × 0.3 mm pellet was used for conductivity measurements. The polymer, ground in a mortar and pestle, was transferred to a pellet die and pressed at 3500 kg/cm^2 under vacuum. Electrodag was applied on the probes for better contact. This apparatus was used to measure the conductivity at 21–22 °C.

The temperature dependence of conductivity was studied from 150 to 500 K by using a sandwich-type two-electrode configuration under dry nitrogen gas for efficient heat transfer. Electrodag was painted on both surfaces of the pellet to elminate contact problems. The apparatus was immersed in a liquid nitrogen–dry ice bath for the low-temperature measurements. Sufficient time was taken to raise the temperature (+10 K/h) to keep the temperature homogeneous. Above room temperature, the Thermo-O-Watch L6-1000 SS temperature controller (Instruments for Research and Industry, Cheltenham) was used to regulate the temperature.

The conductivity measured at 21 °C by the two-electrode probe averaged about 20% lower than that measured by using the four-point probe for all the polymer samples. Therefore, contact resistance was not a problem for these materials and the two-electrode probe measurements should be reliable.

The pressure dependence of conductivity was studied by using a sandwich-type apparatus. Finely ground polymer powder (1.0 g) was put into an insulator, a Teflon washer with a 1.3-cm-diameter and 0.5-cm-thick hole. Riehle M. C.-300 compression testing machine (American Machine and Metals, Inc.) was used to press the powder on opposite sides with two blocks of stainless steel which were connected to a constant current supply and a voltmeter.

Results

It was shown in the previous paper[13] that large numbers of rings still remain open or unoxidized in PMQ1; the majority, but not all, of the rings were fused in PMQ2 and PMQ3, and almost all rings were condensed in PMQ4.

X-ray Diffraction and IR Spectra. Figure 1 shows X-ray diffractions of pristine and NFP-doped PMQ3. The upper spectra correspond to heavier NFP doping. The large band from the layer diffraction progressively shifted from 2θ = 25.9° for pristine PMQ3 to 2θ = 23.3° for the saturated doped PMQ3 (0.69 PF_6^- per repeat unit); the d-spacing increased from 3.34 Å to only 3.82 Å. No intercalation can have occurred during NFP doping. If there were intercalation, the original peak would disappear to be replaced by another at much larger d-spacing, as was found for iodine doping (to be discussed later).

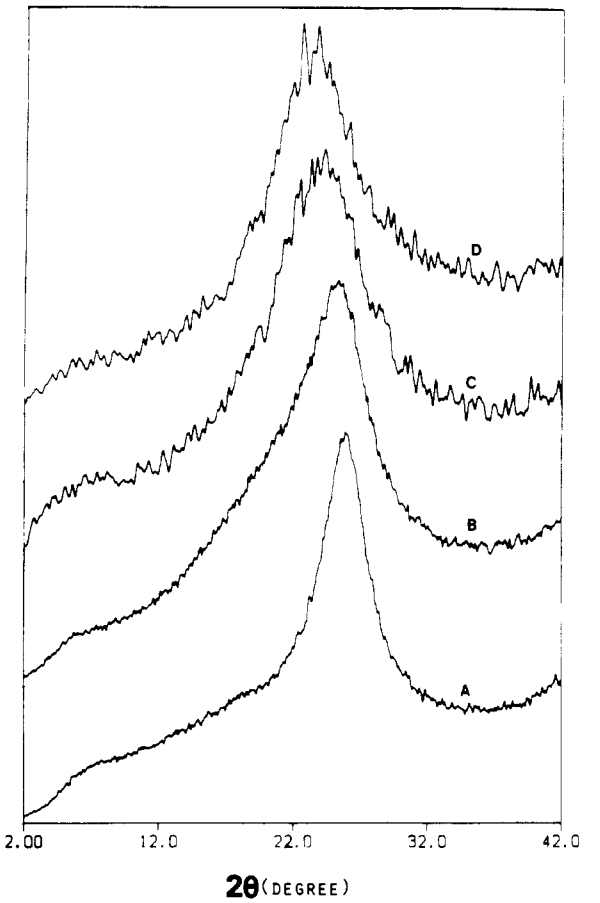

Figure 1. X-ray diffraction of pristine and NFP doped PMQ3: (A) from pristine PMQ3; (B) from lightly doped PMQ3; (C) from medium doped PMQ3; (D) from heavily doped PMQ3.

Since the polymer molecules are stacked in one dimension with the aromatic planes in contact, as shown by the 3.45-Å spacing, if there is no intercalation the PF_6^- group must be packed adjacent to the stack. These stacks are about six molecules thick;[13] the PF_6^- group could be packed on one side of the stack and along the faces of the top and bottom molecules to achieve a ratio of 0.7PF_6^-/residue. They could also be packed on both sides of the stack. The first hypothesis could lead to the observed increase in d-spacing with increased doping as PF_6^- accumulates at the top and bottom of the stack. The PF_6^- group has a van der Waals radius of about 2.94 Å;[19] one can easily calculate a d-spacing for a stack of six PMQ molecules (d = 3.45 Å) coated at top and bottom with PF_6^- groups. This comes to 3.8 Å, which agrees with the experimental value.

X-ray diffraction of saturated iodine-doped PMQ3 (1.14 I per repeat unit) shows an almost complete loss of the peak at 2θ = 26° (3.45 Å) and the generation of a new broad peak at $2\theta \simeq 6°$ (15 Å) (Figure 2). The destruction of the original layer structure combined with the generation of a new larger spacing is probably due to the large amount of iodine intercalation. It has been found that dopant intercalation is facilitated in a planar structure,[20] because of the weak interplanar interaction. This phenomenon has been reported for a wide variety of atomic and molecular species intercalated between the hexagonal carbon monolayers of graphite.[21–23]

Figure 3 shows the IR spectra of NFP-doped PMQ3. The lower spectra correspond to heavier NFP doping. The aromatic C=C and C=N vibration modes shift to higher frequency, from 1595 cm^{-1} for pristine PMQ3 to 1617 cm^{-1} for heavily doped PMQ3. The same phenomenon was also observed in iodine-doped PMQ3, where the band shifted

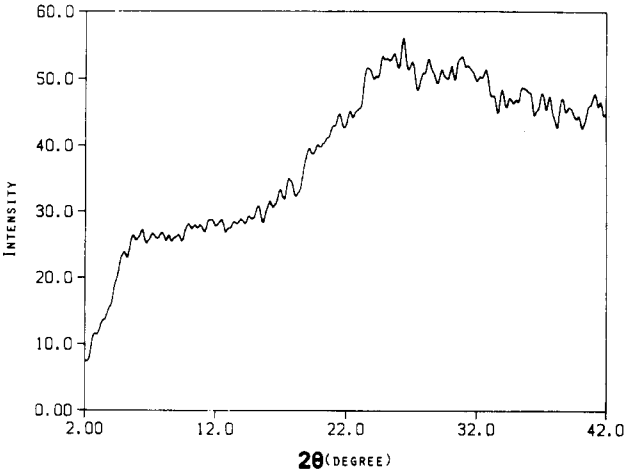

Figure 2. X-ray diffraction of iodine-doped PMQ3.

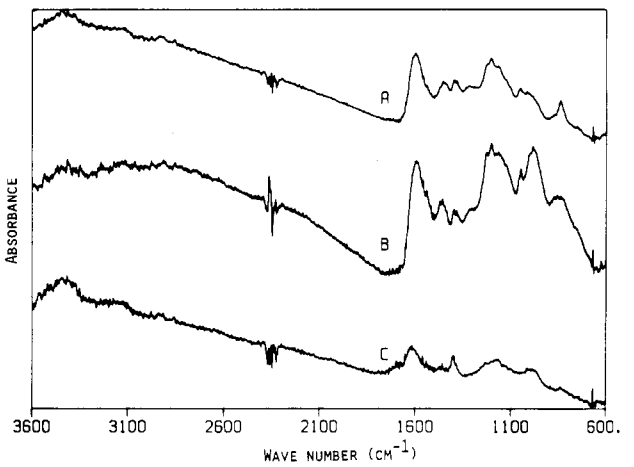

Figure 3. IR spectra of NFP-doped PMQ3: (A) from lightly doped PMQ3; (B) from medium doped PMQ3; (C) from heavily doped PMQ3.

to 1610 cm^{-1} (Figure 4). This is attributed to an increase of the force constants for C=C and C=N bonds due to complexation with the acceptors.[24] The 845-cm^{-1} peak arises from the PF_6^- ion[25] and is present in the spectra of all the doped polymers. There is no peak in this region for the undoped polymer.[13] The broadness of the absorption bands of the bottom spectrum in Figure 3 may be due to plasma electron absorption; significant amounts of free carriers were induced by the heavy doping.

Electron Paramagnetic Resonance. It has been known for a long time that paramagnetic centers are present in conjugated polymers such as *trans*-polyacetylene.[26-28] Unpaired spins can be induced through either thermoexcitation or defects due to, e.g., isomerization. Figure 5 illustrates the temperature dependence of unpaired spin concentration for PMQ1, PMQ2, and PMQ3. At lower temperatures, the spin concentration remains constant but at higher temperatures increases exponentially as temperature increases. The same phenomenon was reported for TCNQ salts[29] and was explained by a single-triplet model.[30] As temperature decreases less electrons can be thermally excited and Curie-type spins (trapped spins) from neutral defects become more and more important. Consequently the spin concentration becomes independent of temperature at lower temperatures. The data were therefore fitted by using eq 3, n_1

$$n = n_1 + n_2 \exp(-\Delta E_1/KT) \quad (3)$$

being the Curie-like spin concentration, n_2 is the total

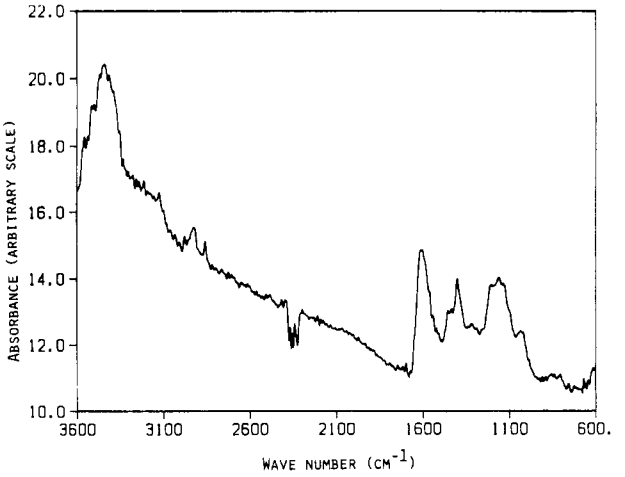

Figure 4. IR spectrum of iodine-doped PMQ3.

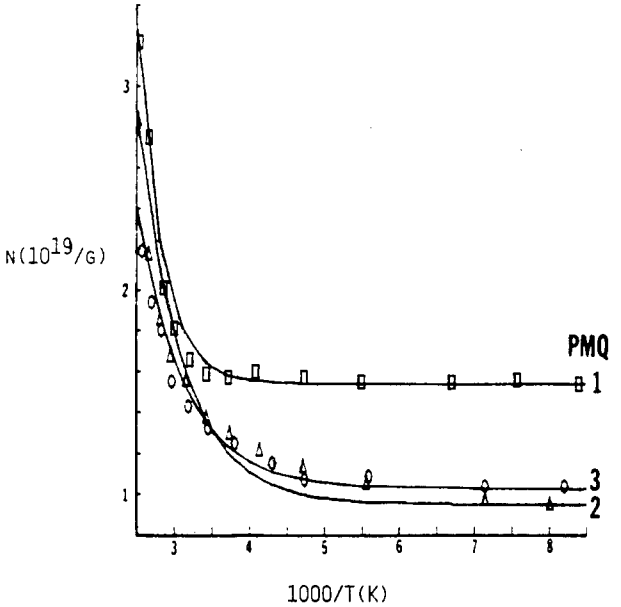

Figure 5. Temperature dependence of the unpaired spin concentration of PMQ1: (1) from PMQ1; (2) from PMQ2; (3) from PMQ3.

potential thermoexcited spin concentration, and ΔE_1 is excitation energy.

PMQ4 behaved very differently from the less condensed members of the series. A lower temperatures, its spin concentration increased as temperature decreased, as illustrated in Figure 6. The reason for this is presently unknown. One possibility is that a phase transition from magnetic disorder to order could occur below a critical temperature, T_c. If this is true, it may appear as either ferromagnetism due to the very large density of states at the Fermi energy,[12] or antiferromagnetism, because of the spin–wave distorted ground states[11,31,32] below T_c. Baldo et al.[32] and S, Kivelson et al.[11] reported that either ferromagnetism or antiferromagnetism would appear for a long enough linear polyacene chain, which is consistent with our result[13] that PMQ4 possesses much longer condensed ring sections than the other three polymers. Intrinsic viscosity of the prepolymer implies that its $\bar{D}\bar{P}_n$ is between 40 and 100.[13]

Three determinations of spin concentration versus temperature for PMQ4 were carried out with reproducible results within experimental error. The data were fitted by using the RS1 computer program with eq 4.

$$n = n_1/(1 - T_c/T) + n_2 \exp(-\Delta E_1/KT) \quad (4)$$

Table II
g Factor, Line Width, Spin Concentration, and Excitation Energy of Pristine PMQ's

PMQ	g	ΔH_{pp}, G	n_{25}, 10^{19}/g	n_1, 10^{19}/g	n_2, 10^{19}/g	ΔE_1, eV
PMQ1	2.0028	11.8	1.58	1.54 ± 0.02	5300 ± 3600	0.275 ± 0.019
PMQ2	2.0028	7.8	1.39	0.95 ± 0.04	130 ± 100	0.146 ± 0.019
PMQ3	2.0028	8.1	1.39	1.03 ± 0.03	72 ± 71	0.136 ± 0.021
PMQ4	2.0028	4.0	3.54	1.86 ± 0.08	96 ± 35	0.104 ± 0.056

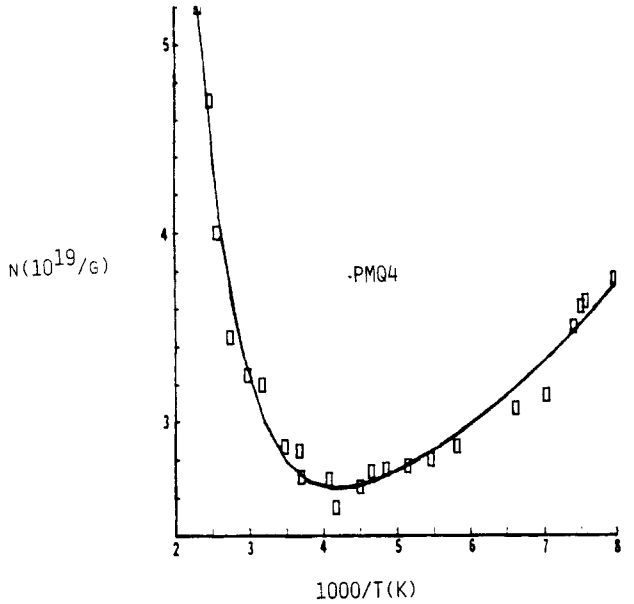

Figure 6. Temperature dependence of the unpaired spin concentration of PMQ4.

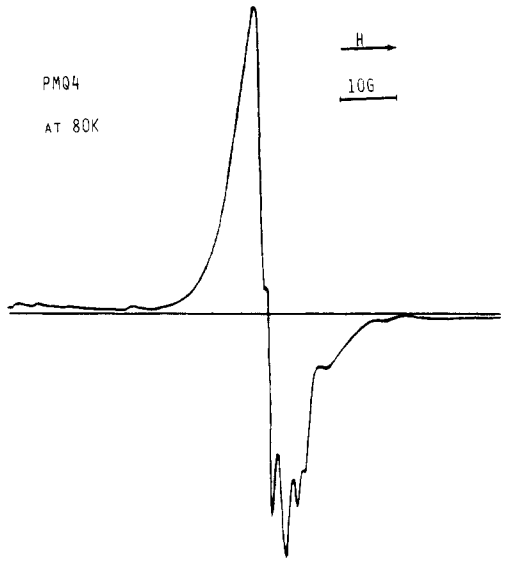

Figure 7. EPR line shape of PMQ4 at 80 K.

The critical temperature, T_c = 74 K, averaged from three data fittings, is close to liquid nitrogen temperature. Exhaustive efforts were made to cool down to T_c for EPR measurement. Fine structure was observed in the range of 79 K (the lowest temperature which could be reached) to 85 K (Figure 7), but it is not certain whether the anomalous peaks are from a new phase. However, the novel spectrum has been reproduced by Dr. H. Kuska, University of Akron, so it is probably real. The extra structure could also be attributed to resolution of g-anisotropy and/or signals from different spin centers. However, PMQ3 does not show this transition down to 77 K.

The g factors; line widths; H_{pp} at room temperature; spin concentrations n_{25}, n_1, and n_2; and ΔE_1 are compiled in Table II.

The major contribution to the EPR signal at room temperature is from Curie-like trapped spins, which are associated with localized carriers.[33] The high excitation energy, ΔE_1, and broad line width of PMQ1 show the effect of short conjugated sequences.

The EPR line shape for undoped polymer can be fitted to a Lorentzian line shape up to five half-line widths, within experimental error. The g factor, 2.0028, is normal for spins in the g-systems of conjugated polymers. There is no effect on g value and line shape and only a slight increase of peak heights upon exposure to air. The effect is reversible. It suggests a weak interaction between polymer and oxygen.

Figure 8 gives the temperature dependence of line width. The line width of PMQ4 is significantly narrower than those of the other three, indicating the spins in PMQ4 are much more mobile. Similarly, the broader line width of PMQ1 suggests that the spins in PMQ1 are more localized, which agrees with the above discussion. Line widths are constant as temperature increases up to about 0 °C. Above this temperature, the lines narrow. The increase of the

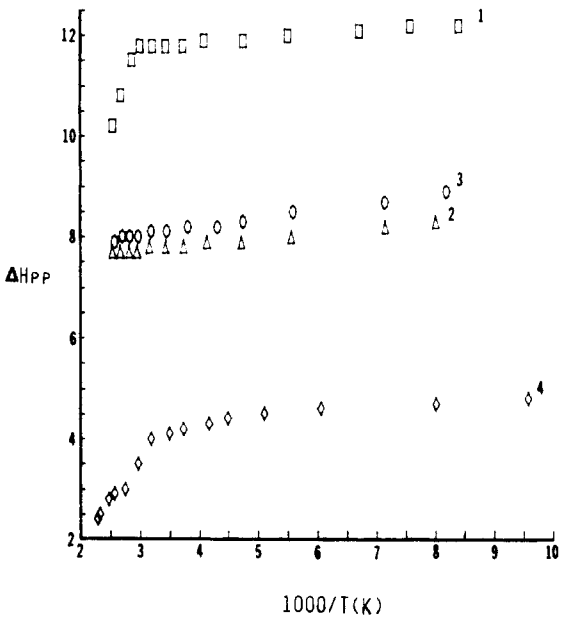

Figure 8. Temperature dependence of line width of pristine polymers: (1) from PMQ1; (2) from PMQ2; (3) from PMQ3; (4) from PMQ4.

spin density accompanied by a decrease of the line width suggests that exchange is the most important mechanism for narrowing of the line width.

The EPR saturation behavior of PMQ3 at room temperature (Figure 9) shows that the maximum amplitude of signal, Y_m', is reached at a microwave power of about 5 mW. The saturation value, H_{1m}, corresponding to the maximum signal, can be used to calculate the spin–lattice relaxation time, T_1, and spin–spin relaxation time, T_2.[34]

$$T_1 = 0.49 \times 10^{-7}\ \Delta H^\circ_{pp}/(g(H_{1m})^2)\ \text{s} \quad (5)$$

$$T_2 = 1.313 \times 10^{-7}/g\Delta H^\circ_{pp}\ \text{s} \quad (6)$$

ΔH°_{pp} is the smallest line width below saturation. At high

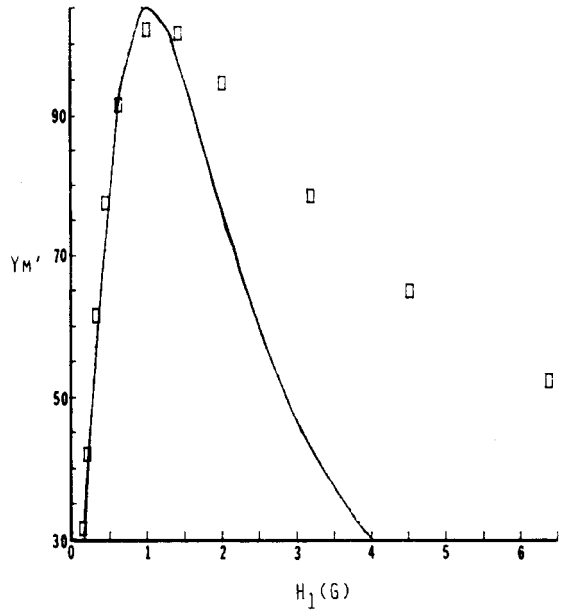

Figure 9. EPR saturation of PMQ3 at room temperature.

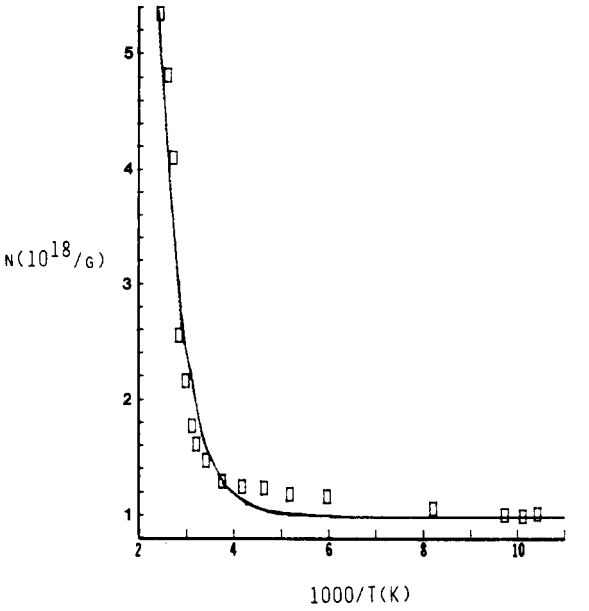

Figure 10. Temperature dependence of unpaired spin concentration of NFP-doped PMQ3.

Table III
Relaxation Times T_1 and T_2 of Pristine Polymer

PMQ	T_1, 10^{-5} s	T_2, 10^{-9} s	PMQ	T_1, 10^{-5} s	T_2, 10^{-9} s
PMQ1	3.5	5.6	PMQ3	10.5	8.1
PMQ2	14.7	8.9	PMQ4	3.4	16.4

power levels, the signal, Y_m', decreases more slowly than predicted theoretically by eq 7,[34] where $z = \gamma H_1(T_1T_2)^{1/2}$.

$$Y \sim z/(1 + z^2)^{3/2} \quad (7)$$

This may indicate inhomogeneous saturation and/or may result from the linear increase of the sample temperature with power. However, Gaussian line shape should be expected if it is inhomogeneously broadened. The observed Lorentian line shape makes the inhomogenously broadening unlikely. T_1 and T_2 are listed in Table III.

Upon exposure to air, T_1 was reduced slightly (~10%) for all pristine polymers; T_2 did not change detectably.

After doping PMQ3 with NFP, there is no visible effect on line shape, except a slight shift of g value and reduction of line width, from 8.1 to 5.4 G, at room temperature. The excitation energy obtained from variable-temperature unpaired spin data (Figure 10) increases slightly (Table IV). However, there is significant decrease of the spin concentration, 10.5-fold for Curie spins and 5.4-fold for thermoexcited spins, which indicates that NO^+ oxidized Curie spins to spinless cations as well as generating bipolarons.

Variable-temperature unpaired spin concentration data for iodine-doped PMQ3 cannot be fitted satisfactorily by eq 3. Plotting the signal intensity, which is proportional to spin susceptibility, versus temperature (Figure 11) shows that the intensity does not vary with n_1/T, instead,

$$I \sim 3n_0/2T_f + n_1/T \quad (8)$$

where n_1 is the Pauli-type spin concentration and T_f is the Fermi temperature, on the order of 10^5 K for most normal nonferromagnetic metals.[35] The fitting was excellent at low temperature. The deviation at high temperature

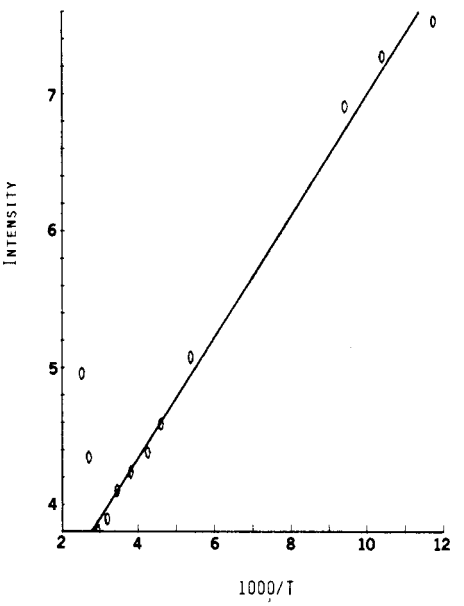

Figure 11. Temperature dependence of EPR intensity of iodine-doped PMQ3.

probably was due to evaporation of iodine under vacuum. This was confirmed by observation that the line shape became more symmetric after cooling. From curve fitting, n_0/T_f is 3.4×10^{16} g^{-1} K^{-1} and n_1 is 9.5×10^{18} g^{-1}. This suggests that a large number of Pauli-like spins, i.e., free carriers, are induced by iodine doping.

The asymmetric line shape (Figure 12), coupled with a shift of the g value to 2.0045 plus its broader line width, also indicates formation of new unpaired spins and strong interaction between the spin system and iodine nuclei.

EPR saturation studies of doped PMQ3 indicate that there is only a slight effect on T_1 for NFP doped PMQ3. The resonance for iodine-doped PMQ3 could not be saturated with the power available. This implies an anom-

Table IV
g Factor, Line Width, Spin Concentration, and Excitation Energy of NFP- and Iodine-Doped PMQ3

PMQ	g	ΔH_{pp}, G	$n_{25}°$, 10^{19}/g	n_1, 10^{19}/g	n_2, 10^{19}/g	ΔE_1, eV
PMQ3–NFP	2.0031	5.4	0.165	0.098 ± 0.010	54.6 ± 34.7	0.172 ± 0.018
PMQ3–I	2.0045	9.7		0.951 ± 0.089		

Table V
Electronic Conductivity, Activation Energy, and Optical Threshold, E_g', of Pristine Polymer

PMQ	σ_{25}, S/cm	σ_0, S/cm	ΔE, eV	E_g', eV
PMQ1	1.7×10^{-11}	4.1 (+2.1) (−1.4) × 10^4	0.91 ± 0.011	1.0
PMQ2	5.8×10^{-9}	80 (+43) (−28)	0.60 ± 0.011	0.6
PMQ3	7.8×10^{-9}	3.3 (+1.2) (−0.9)	0.51 ± 0.009	0.6
PMQ4	2.1×10^{-5}	1.7 (+0.3) (−0.2)	0.35 ± 0.003	0.3

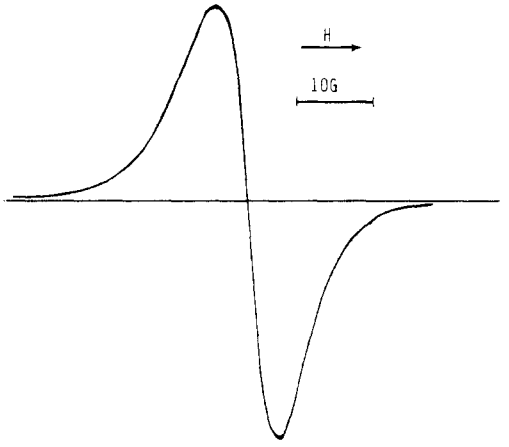

Figure 12. EPR line shape of iodine-doped PMQ3.

alously short relaxation time T_1, probably due to a strong interaction between iodine nuclei and the spin system, which is consistent with the above data. The tighter the coupling of the spin system and the dopant nuclei, the quicker the recovery from magnetic disturbance, and the smaller T_1 becomes.

The data for g value, ΔH_{ppm}, $n_{25}°$, n_1, n_2, and ΔE_1 of both NFP and iodine doped PMQ3 are summarized in Table IV.

Electronic Conductivity. The electronic conductivities at room temperature are on the order of 10^{-11} S/cm for pristine PMQ1, and 10^{-9} S/cm for PMQ2 and PMQ3. The conductivity of PMQ4, however, is 2.1×10^{-5} S/cm, which is about 1 order of magnitude higher than that of PPMQ,[17] as expected. After saturation doping of PMQ3 with NFP and iodine, the conductivity at 21 °C increases to 1.3×10^{-3} and 2.4×10^{-2} s/cm, respectively. This is of the same order as that of iodine-doped PPMQ.[17]

Temperature/conductivity plots for the pristine polymers normalized to the room temperature conductivity are given in Figure 13. They exhibit a thermally activated temperature dependence

$$\sigma = \sigma_0 \exp(-\Delta E/KT) \quad (9)$$

where ΔE is the activation energy. σ_{25}, and the calculated σ_0, and ΔE are listed in Table V. An increase of condensation temperature results in decrease of the activation energy. The optical absorption thresholds of PMQ's obtained from UV/vis absorbance versus wavenumber and extrapolating to zero are also listed in Table V.[13] It is interesting that the activation energy for each polymer is about equivalent to its threshold, E_g', the bandgap between the top of valence band and the bottom of conduction band.

Figure 14 displays the temperature dependence of conductivity for NFP-doped PMQ3. The high-temperature (150 °C) "bendover" might be due to decomposition of the dopant as is seen in doped poly(*p*-phenylene sulfide).[36] In the temperature range −10 to 150 °C, the data follow normal thermal activation, eq 7. The corresponding activation energy, 0.17 eV, is one-third of that for pristine PMQ3, which could be due to the formation of bipolarons[37] after doping. This is strongly suggested by the significant

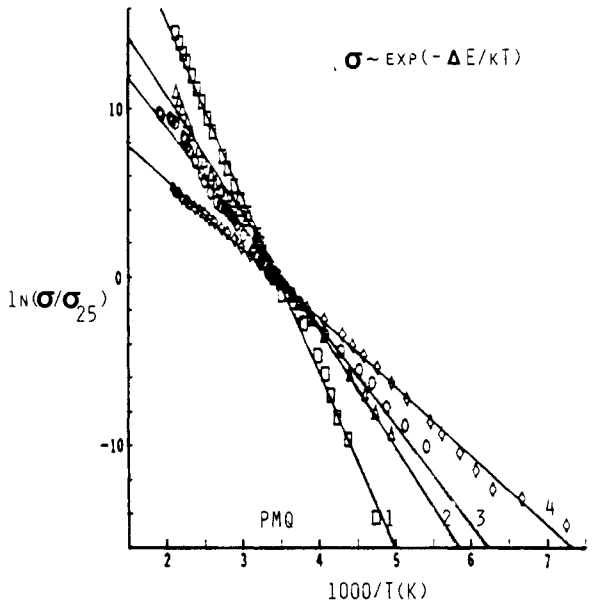

Figure 13. Temperature dependence of conductivity for pristine PMQ: (1) from PMQ1; (2) from PMQ2; (3) from PMQ3; (4) from PMQ4.

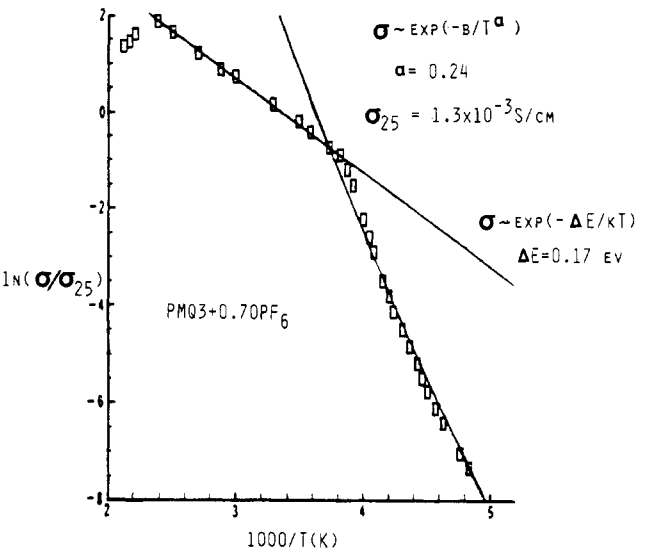

Figure 14. Temperature dependence of conductivity of NFP-doped PMQ3.

reduction of unpaired spins after doping PMQ3 with NFP. However, at temperatures below −10 °C, the conductivity data can be fitted satisfactorily by either eq 10 or eq 11.

$$\sigma \sim \exp(-a/T^{1/2}) \quad (10)$$

$$\sigma \sim \exp(-b/T^{1/4}) \quad (11)$$

Equation 10 is based on a model of tunneling in metallic grains with a square potential barrier.[38,39] It holds only a sufficiently low field and metallic domain concentration below the percolation threshold. In contrast, eq 11 is only valid for concentrations well above the percolation threshold; charge transport is characterized as a three-

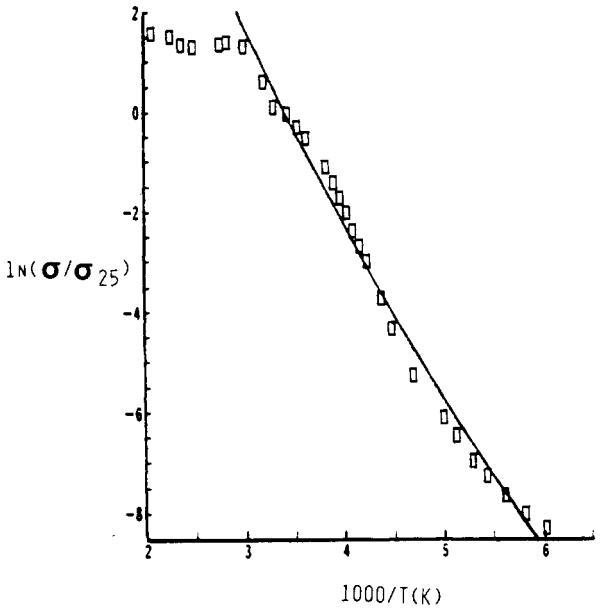

Figure 15. Temperature dependence of conductivity of iodine-doped PMQ3.

dimensional variable range hopping near the Fermi energy.[40,41] At this point, one cannot choose between these two models. Nevertheless, the best fit, from nonlinear least-square refined refinement analysis (RS1 computer program) is to eq 12, where $\alpha = 0.24 \pm 0.14$. This value

$$\sigma \sim \exp(-b/T^{\alpha}) \tag{12}$$

of α is closer to one-quarter than to one-half.

The temperature conductivity data of iodine-doped PMQ3 (Figure 15) can be fitted not only to eq 11 but also to a model of fluctuation-induced carrier tunneling through potential barriers separating metallic regions (eq 13).[42-44]

$$\sigma = \sigma_0 \exp(-T_1/(T + T_0)) \tag{13}$$

Here T_1 refers to an effective barrier activation energy and T_0 is a parameter depending on barrier height, V_0; thickness, W; and cross-section, A. They are defined in eq 14 and 15.

$$T_1 = (2AV_0^2)/(\pi e^2 KW) \tag{14}$$

$$T_0 = (4hAV_0^{1/2})/(\pi e^2 KW^2(2m)^{1/2}) \tag{15}$$

Again, it is difficult to choose between these two mechanisms from the data. In any case, both suggest that a high metallic domain concentration was induced by iodine doping.[42]

The stack packing is definitely retained for the NFP-doped polymer; while intercalation of iodine probably does not destroy the stack structure, it separates the molecules. As was pointed out, the stacks are bent into arcs or cylinders which cannot pack efficiently. Thus the models of conducting domains with high potential barriers between the domains are appropriate for these materials. The conductivity behavior is compatable with the structure.

Figure 16 shows the pressure dependence of conductivity for both NFP-doped and pristine PMQ3. The conductivity increased as pressure increased for both the polymers until the pressure reached 3.0×10^4 kg/cm^2, indicating electronic conduction, because ionic conductivity decreases as pressure increases.[45] However, the conductivity of the doped PMQ3 decreased as pressure increased further. This was an experimental artifact. The sample integrity was destroyed; the conductivity decreased about 20-fold after releasing the high pressure.

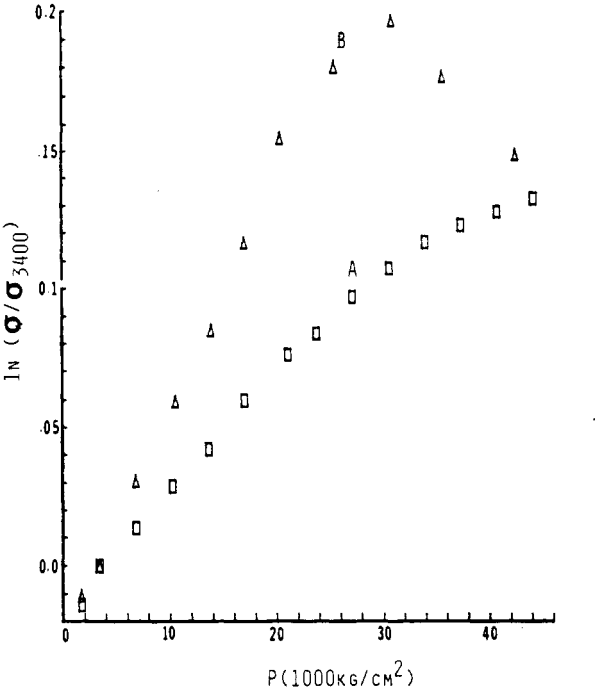

Figure 16. Pressure dependence of conductivity of pristine and NFP-doped PMQ3: (A) from PMQ3; (B) from doped PMQ3.

Discussion

EPR studies show that two kinds of unpaired spins exist in PMQ: Curie spins and thermally excited spins. Curie spins are delocalized over many residues, as shown by their narrow line widths, but are isolated from other Curie spins; the thermally excited spins correspond to polarons. The percentage contribution of trapped spins to the EPR signal at room temperature, the unpaired spin excitation energy, carrier activation energy, and the absorption threshold all decrease as reaction temperature increases, which shows that higher temperature condensation generates a polymer with longer conjugated sequences. The narrowing of the p–p width of the EPR signals above room temperature shows that thermally excited spins can exchange with the trapped spins.

NO^+ oxidizes the Curie spins to spinless cations and polarons and π-electrons to bipolarons, which might be the main contributors to charge carriers in the NFP-doped PMQ3. Iodine intercalation is promoted by charge transfer with strong interaction between the iodine nuclei and the π-electrons. This creates new spins (polarons) as well as oxidizing the Curie spins. The observed Pauli spins and very short spin–lattice relaxation times are consistent with the above interpretation.

Electronic conductivity for undoped PMQ4 of 2.1×10^{-5} S/cm is quite high. The moderate level of impurity, H_2SO_4, which was found in other PMQ's may affect the conductivity, i.e., conductivity is not intrinsic. This is supported by the experimental result that the conduction activation energy for a given PMQ is roughly equivalent to its optical threshold energy. Half the threshold energy is expected for the activation energy if conductivity is intrinsic.[45]

The room temperature conductivity of iodine-doped PMQ3, 2.4×10^{-2} S/cm, is not very impressive. The question arises whether interparticle or interstack contact resistance controls its conductivity. The very weak pressure dependence of conductivity indicates that interparticle contacts are not as important as interstack contacts. Therefore one should not expect a high, metallic conductivity; this is also true for AsF_5-doped *cis*-polyacetylene.[46]

Because the molecular stacks of PMQ are arcs or cylinders, they cannot pack closely. Thus while the carrier mobility may be very high within a stack, the interstack mobility is low. It is difficult for current carriers to tunnel through the interstack potential barrier; consequently, the conductivity is low.

The EPR data for PMQ4 is very unusual. The increase in observed n (signal intensity times temperature) can be rationalized in several ways. We favor the hypothesis that the polymer approaches a magnetic transition as the temperature lowers with a T_c of about 74 K. The increase in signal in this view is due to increasing spin–spin interactions as the temperature lowers, increasing the effective spin dipole and thus the response.

This view that the spins respond well to magnetic fields is supported by some results on PMQ4 reported to us by Dr. Hatfield, University of North Carolina, Chapel Hill. He measured the magnetic susceptibility of the polymer at 10000 Oersteds from 4 to 300 K and found it independent of temperature. The spins were saturated. (This will be reported more fully separately.) This result cannot be explained fully at present, but it shows that the spins respond very strongly to a strong magnetic field.

Conclusions

Significant differences were observed in EPR and conductivity studies for PMQ1, PMQ2, PMQ3, and PMQ4. Narrow line width plus strong temperature dependence of PMQ4 indicates high spin mobility, which is consistent with its high conductivity, 2.1×10^{-5} S/cm. PMQ3 doped with NFP and iodine became electrically conducting, σ_{25} was 1.3×10^{-3} and 2.4×10^{-2} S/cm, respectively. NFP doping oxidized the π-electron system, destroying most of the spins. Iodine doping caused the destruction of the layer structure through intercalation, and created Pauli-like free carriers. There is a distinction between unpaired spins and charged carriers: Curie spins are trapped paramagnetic species but not current carriers; bipolarons can carry charges by hopping, in much the same way as polarons, except that they are doubly charged and diamagnetic. At high doping levels, conduction may occur via tunneling through interstack potential barriers.

High-temperature condensed PMQ4 is clearly the most interesting material. There is a possible phase transition from magnetic disorder to order for PMQ4 near 74 K. The main stumbling block for studying this material is its insolubility; it is very difficult to separate the polymer from impurity. A study to improve synthetic procedures and the investigation of the magnetic properties of PMQ is well worthwhile.

Acknowledgment. Stimulating discussions with Dr. W. L. Gordon are greatly appreciated. This work was partly supported by Dow Chemical Co., DOE, and the National Science Foundation.

Registry No. PMQ, 104491-01-2; NFP, 16921-91-8; I_2, 7553-56-2; (2,6-$(H_2N)_2C_6H_3CH_3$)(CH_2O) (copolymer), 112265-13-1.

References and Notes

(1) Street, G. B.; Clarke, T. C. *IBM Res. Dev.* **1981**, *25*, 51.
(2) Clarke, T. C.; Kanazawa, K. K.; Lee, V. Y.; Rabolt, Y. F.; Reynolds, J. R.; Street, G. B. *J. Polym. Sci., Polym. Phys. Ed.* **1982**, *20*, 117.
(3) Lerner, N. R. *Polymer* **1983**, *24*, 800.
(4) Jenekhe, S. A.; Wellinghoff, S. T.; Reed, J. F. *Mol. Cryst. Liq. Cryst.* **1984**, *105*, 175.
(5) Peierls, R. E. *Quantum Theory of Solids*; Clarendon: Oxford, 1955; p 108.
(6) Rice, M. J.; Strasler, S. *Solid State Commun.* **1975**, *13*, 125.
(7) Scott, A. C.; Chu, F. Y. F.; McLaughlin, D. W. *Proc. IEEE* **1973**, *61*, 1443.
(8) Su, W. P.; Schrieffer, J. R.; Heeger, A. J. *Phys. Rev. Lett.* **1979**, *42*, 1698; *Phys. Rev. B: Condens. Matter* **1980**, *22*, 2099.
(9) Kittel, C. *Introduction to Solid State Physics*; Wiley: New York, 1976; pp 230–231.
(10) Salem, L.; Longuet-Higgins, H. C. *Proc. R. Soc. London, A* **1960**, *255*, 435.
(11) Kivelson, S.; Chapman, O. L. *Phys. Rev. B: Condens. Matter* **1983**, *28*, 7236.
(12) Baldo, M.; Piccitto, G.; Pucci, R.; Tomasello, P. *Phys. Lett. A* **1983**, *95A*, 201.
(13) Ruan, J. Z.; Litt, M. H. *Macromolecules*, preceding paper in this issue.
(14) Tanaka, K.; Ohzeki, K.; Nankai, S.; Yamabe, T.; Shirakawa, H. *J. Phys. Chem. Solid* **1983**, *44*, 1069.
(15) Courley, K. D.; Lillya, C. P.; Reynolds, C. R.; Chien, J. C. W. *Macromolecules* **1984**, *17*, 1025.
(16) Freed, J. H.; Leniart, D. S.; Hyde, J. S. *J. Chem. Phys.* **1967**, *47*, 2762.
(17) Ruan, J. Z.; Litt, M. H. *J. Polym. Sci., Polym. Chem. Ed.* **1987**, *25*, 285.
(18) Wasscher, J. D. *Philips Res. Rep.* **1961**, *16*, 301.
(19) Toy, A. D. F.; O'Donnell, T. A. In *Comprehensive Inorganic Chemistry*; Trotman-Dickenson, A. F., Ed.; Pergamon: New York, 1973; Vol. 2, pp 422 and 1021.
(20) Tripathy, S. K.; Kitchen, D.; Druy, M. A. *Polym. Prepr. (Am. Chem. Soc., Div. Polym. Chem.)* **1982**, *23*, 109.
(21) Fischer, J. E. *Mater. Sci. Eng.* **1977**, *31*, 211.
(22) Fouletier, M.; Degott, P.; Armand, M. *Solid State Ionics* **1983**, *8*, 165.
(23) Platts, D. D. A.; Chung, D. D. L.; Dresselhaus, M. A. *Phys. Rev. B: Condens. Matter* **1977**, *15*, 1087.
(24) Kim, O. K. *J. Polym. Sci., Polym. Lett. Ed.* **1985**, *23*, 137.
(25) Brant, P.; Nohr, R. S.; Wynne, K. J.; Weber, J. D. C. *Mol. Cryst. Liq. Cryst.* **1982**, *81*, 255.
(26) Shirakawa, H.; Ito, T.; Ikeda, S. *Macromol. Chim.* **1978**, *179*, 1565.
(27) Goldberg, I. B.; Crowe, H. R.; Newman, P. R.; Heeger, A. J.; MacDiarmid, A. G. *J. Chem. Phys.* **1979**, *70*, 1132.
(28) Snow, A.; Brant, P.; Weber, D. *J. Polym. Sci., Polym. Lett. Ed.* **1979**, *17*, 263.
(29) Rembaum, A.; Hermann, A. M.; Stewart, F. E.; Gutmann, F. *J. Phys. Chem.* **1969**, *73*, 513.
(30) Biji, D.; Kainer, H.; Rose-Inns, A. C. *J. Chem. Phys.* **1959**, *30*, 765.
(31) Fukutome, H. *Prog. Theor. Phys.* **1968**, *40*, 998.
(32) Baldo, M.; Grassi, A.; Pucci, R.; Tomassello, P. *J. Chem. Phys.* **1982**, *77*, 2438.
(33) Weinberg, B. R.; Kanfer, J.; Heeger, A. J.; Pron, A.; MacDiarmid, A. G. *Phys. Rev. B: Condens. Matter* **1979**, *20*, 223.
(34) Poole, C. P., Jr. *Electron Spin Resonance*; Wiley: New York, 1983; pp 589–595.
(35) Ashcroft, N. W.; Mermin, N. D. *Solid State Physics*; Holt, Rinehart and Winston: New York, 1983; p 38.
(36) Rubner, M.; Cukor, P.; Jopson, H.; Deits, W. *J. Electron. Mater.* **1982**, *11*, 261.
(37) Scott, J. C.; Pfluger, P.; Kronubi, M. T.; Street, G. B. *Phys. Rev. B. Condens. Matter* **1983**, *28*, 2140.
(38) Sheng, P.; Abeles, B.; Arie, Y. *Phys. Rev. Lett.* **1973**, *31*, 44.
(39) Abeles, B.; Sheng, P.; Coutts, M. D.; Arie, Y. *Adv. Phys.* **1975**, *24*, 407.
(40) Epstein, A. J.; Rommelmann, H.; Abkowitz, M.; Gibson, H. W. *Mol. Cryst. Liq. Cryst.* **1981**, *77*, 81.
(41) Audenaert, M.; Gusman, G.; Rellour, R. *Phys. Rev. B: Condens. Matter* **1981**, *24*, 7380.
(42) Sheng, P.; Sichel, E. K.; Gittleman, J. I. *Phys. Rev. B: Condens. Matter* **1978**, *18*, 1197.
(43) Sichel, E. K.; Gittleman, J. I.; Sheng, P. *Phys. Rev. B: Condens. Matter* **1978**, *18*, 5712.
(44) Park, Y. M.; Heeger, A. J.; Druy, M. A.; MacDiarmid, A. G. *J. Chem. Phys.* **1980**, *73*, 946.
(45) Blythe, A. R. *Electronic Propertiesof Polymers*; Cambridge University Press: New York, 1979; pp 96 and 101.
(46) Tomkiewicz, Y.; Schultz, T. D.; Brom, H. B.; Taranko, A. R. *Phys. Rev. B: Condens. Matter* **1981**, *24*, 4348.